The EMBO Journal (2009), 1–14 | © 2009 European Molecular Biology Organization | All Rights Reserved 0261-4189/09
www.embojournal.org

THE EMBO JOURNAL

MDM4 (MDMX) localizes at the mitochondria and facilitates the p53-mediated intrinsic-apoptotic pathway

Francesca Mancini[1,2], Giusy Di Conza[1,3], Marsha Pellegrino[1], Cinzia Rinaldo[4], Andrea Prodosmo[2,4], Simona Giglio[1,2], Igea D'Agnano[1], Fulvio Florenzano[5], Lara Felicioni[6], Fiamma Buttitta[6], Antonio Marchetti[6], Ada Sacchi[4], Alfredo Pontecorvi[2], Silvia Soddu[4] and Fabiola Moretti[1,*]

[1]Institute of Neurobiology and Molecular Medicine, National Council of Research, Rome, Italy, [2]Division of Endocrinology, Catholic University, Rome, Italy, [3]Department of Experimental-Clinical Medicine and Pharmacology, University of Messina, Messina, Italy, [4]Molecular Oncogenesis Laboratory, Regina Elena Cancer Institute, Rome, Italy, [5]Confocal Microscopy Unit, EBRI-CNR-Fondazione Santa Lucia, Rome, Italy and [6]Clinical Research Center, University-Foundation 'G D'Annunzio', Chieti, Italy

MDM4 is a key regulator of p53, whose biological activities depend on both transcriptional activity and transcription-independent mitochondrial functions. MDM4 binds to p53 and blocks its transcriptional activity; however, the main cytoplasmic localization of MDM4 might also imply a regulation of p53-mitochondrial function. Here, we show that MDM4 stably localizes at the mitochondria, in which it (i) binds BCL2, (ii) facilitates mitochondrial localization of p53 phosphorylated at Ser46 (p53Ser46^P) and (iii) promotes binding between p53Ser46^P and BCL2, release of cytochrome C and apoptosis. In agreement with these observations, MDM4 reduction by RNA interference increases resistance to DNA-damage-induced apoptosis in a p53-dependent manner and independently of transcription. Consistent with these findings, a significant down-regulation of *MDM4* expression associates with cisplatin resistance in human ovarian cancers, and MDM4 modulation affects cisplatin sensitivity of ovarian cancer cells. These data define a new localization and function of MDM4 that, by acting as a docking site for p53Ser46^P to BCL2, facilitates the p53-mediated intrinsic-apoptotic pathway. Overall, our results point to MDM4 as a double-faced regulator of p53.

The EMBO Journal advance online publication, 11 June 2009; doi:10.1038/emboj.2009.154

Subject Categories: proteins; differentiation & death

Keywords: BCL2; MDM4 (MDMX); mitochondrial apoptosis; p53

*Corresponding author. Institute of Neurobiology and Molecular Medicine, National Council of Research, Via del Fosso di Fiorano, 64, Roma 143, Italy. Tel.: +39 065 0170 3242; Fax: +39 065 0170 3313; E-mail: moretti@inmm.cnr.it

Received: 22 December 2008; accepted: 18 May 2009

Introduction

MDM4, formerly named MDMX, is an inhibitor of p53 with *in vitro* and *in vivo* oncogenic potential (Marine *et al*, 2006, 2007; Toledo and Wahl, 2006). The relevance of MDM4 regulation of p53 has been established by the *Mdm4* knockout (KO) mice (Parant *et al*, 2001; Finch *et al*, 2002; Migliorini *et al*, 2002a). These animals show embryonic lethality, but have a normal development when simultaneously deleted for *Trp53* gene.

Different models have been proposed to explain the activity of MDM4 towards p53, particularly to distinguish MDM4 from its analogue MDM2, the best characterized negative regulator of p53. As the most evident phenotype of *Mdm4*-KO mice is a generalized cell cycle arrest (Parant *et al*, 2001; Migliorini *et al*, 2002a), MDM4 has been considered as a negative regulator of p53 growth arresting function (Parant *et al*, 2001). Conversely, the control of p53-apoptotic function has been attributed to MDM2 because of the presence of early embryonic cell death in *Mdm2*-KO mice (Jones *et al*, 1995; Montes de Oca-Luna *et al*, 1995). This model, therefore, attributes the control of distinct activities of p53 to different proteins. In contrast to this, a second model is based on the evidence that MDM4 and MDM2 efficiently associate and regulate each other's function. It has been proposed that the interdependence of the two MDM proteins is the basis for the negative non-overlapping regulation of p53 (Gu *et al*, 2002; Wade and Wahl, 2009). The presence of apoptosis in *Mdm4*-KO mice in neuronal progenitors (Migliorini *et al*, 2002a; Francoz *et al*, 2006; Xiong *et al*, 2006), an increased transcription of some p53 targets genes (Francoz *et al*, 2006; Toledo *et al*, 2006; Xiong *et al*, 2006), have raised a third hypothesis: MDM4 controls the transcriptional function of p53, whereas MDM2 controls its protein levels (Francoz *et al*, 2006; Toledo *et al*, 2006). All these models apply mainly to the regulation of p53 in unstressed conditions and/or during the mouse development, although some data also extend them to stressing situations (Toledo *et al*, 2006).

After DNA damage, MDM4 protein levels are downregulated by MDM2-degradative activity (Kawai *et al*, 2003; Pan and Chen, 2003; Pereg *et al*, 2005). The dissociation of deubiquitylating enzyme HAUSP from the MDM4–MDM2 complex is the primary event (Meulmeester *et al*, 2005), whereas the increase in MDM2 levels by p53-mediated transcription reinforces this mechanism (Toledo and Wahl, 2006). In agreement with the model of MDM4 as a negative regulator of p53, these events contribute to the release of p53 activity by MDM4 inhibition.

However, a few data have suggested additional activities of MDM4. Survival and proliferation of mouse embryo fibroblasts (MEFs) overexpressing Mdm2, plated at low density, are suppressed by the presence of Mdm4. Accordingly, the rate of tumour formation is accelerated in Mdm2 transgenic mice lacking both *Mdm4* alleles in comparison to the mice

having both alleles (Steinman *et al*, 2005). Further, both overexpressed and endogenous MDM4 stabilize active p53 by counteracting its MDM2-mediated degradation (Jackson and Berberich, 2000; Stad *et al*, 2000; Barboza *et al*, 2008), and overexpressed MDM4 promotes p53-mediated apoptosis in stressing conditions (Mancini *et al*, 2004). These data suggest a conflicting activity between MDM4 and MDM2 under some circumstances. As on severe genotoxic stress MDM2 levels and/or activity remain low or even decrease (Ashcroft *et al*, 2000; Latonen *et al*, 2001; Marchenko *et al*, 2007; Rinaldo *et al*, 2007), we have investigated the function exerted by MDM4 under these conditions. Particularly, as MDM4 is mainly a cytoplasmic protein, we studied its effect on the cytoplasmic function of p53, specifically the transcription-independent mitochondrial apoptosis.

Here, we show that a fraction of the MDM4 protein stably resides at the mitochondria, in which, on a lethal type of stress, it promotes (i) the recruitment of the p53 phosphorylated on Ser46, (ii) its binding to BCL2 and (iii) the mitochondrial outer membrane permeabilization (MOMP) with release of cytochrome C. Overall, our data point to a novel role of MDM4 as a positive regulator of p53-intrinsic apoptosis.

Results

MDM4 is localized at the mitochondria

MDM4 is mainly a cytoplasmic protein (Migliorini *et al*, 2002b). To determine the MDM4 subcellular localization, we analysed the cell fractions from transient MDM4 reconstituted, $p53^{-/-}Mdm4^{-/-}$MEFs (MDM4^{+}DKO-MEFs) and detected MDM4, but not its analogue MDM2, at the mitochondria (Figure 1A). Analysis of mitochondrial fractions from various cell lines showed that the endogenous protein localizes at these organelles also (Figure 1B). MDM4-mitochondrial fraction to the cytosolic varies from 10% in A2780

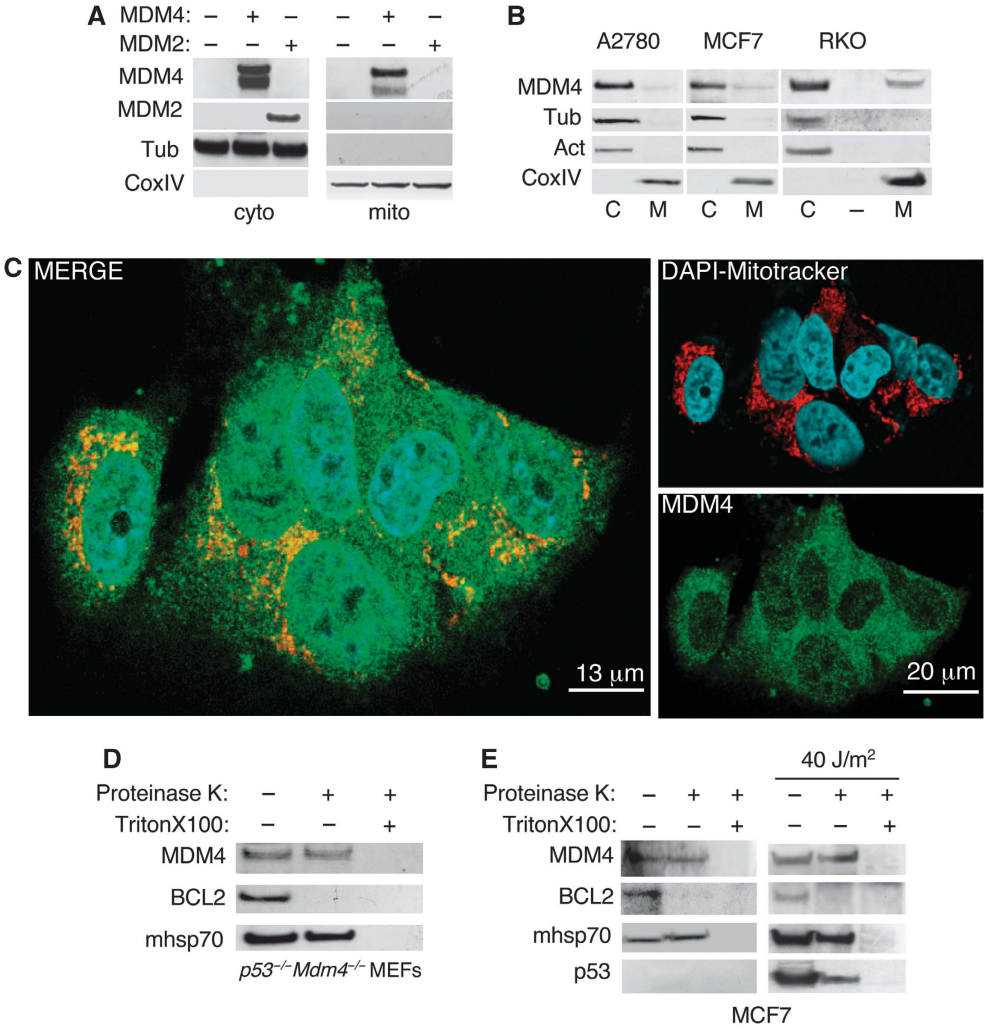

Figure 1 MDM4 is localized in the internal compartments of mitochondria. (**A**) MDM2 and MDM4 were transiently expressed in $p53^{-/-}Mdm4^{-/-}$MEFs. After 24 h, WCEs were subfractionated in cytosolic and mitochondrial fractions by differential centrifugations and analysed by SDS–PAGE. Cytosolic and mitochondrial contamination was verified by a-cyclooxygenase IV (CoxIV) and Tubulin (Tub) used as loading control also. (**B**) Wb analysis of endogenous MDM4 in cytosolic and mitochondrial fractions of indicated human tumour cell lines. Actin (Act) was used as a further loading control and contamination marker. (**C**) Confocal microscopy of indicated signals in MCF7 cells. MDM4 protein shows a prevalent and diffuse cytoplasmatic granular staining with a partial mitochondrial co-localization. MDM4 staining was obtained with anti-MDM4 antibody 6B1A (**D**, **E**) Mitochondrial fractions of $p53^{-/-}Mdm4^{-/-}$MEFs re-expressing MDM4 (D) and MCF7 (E) were enzymatically digested by ProteinaseK in the presence or absence of TritonX100 (1%) and subsequently analysed by Wb. Right panel of (E), MCF7 cells were subjected to UV irradiation (40 J/m^2) and after 8 h mitochondria were isolated and treated as indicated.

to 21% in MCF7, and to 29% in RKO cells. To confirm these biochemical data, immunofluorescence for MDM4 and for a marker that selectively stains mitochondria (MitoTracker Red dye) was performed in MCF7 cells and in MDM4^{+}DKO-MEFs. Merging of the signals by confocal microscopy supported the localization of both the endogenous (Figure 1C) and exogenous MDM4 (Supplementary Figure S1A) at the mitochondria, whereas the control GFP protein did not show a similar localization pattern (Supplementary Figure S1B). To further characterize the association of MDM4 with these organelles, we performed an enzymatic digestion of mitochondrial fractions from MDM4^{+}DKO-MEFs (Figure 1D) and MCF7 cells (Figure 1E). After digestion with proteinase K, a non-specific protease unable to cross the outer mitochondrial membrane (Reef *et al*, 2006), MDM4 was still recoverable in the pellet, whereas BCL2, a protein tail anchored to the mitochondrial membrane, was degraded. MDM4 disappeared only after treatment of mitochondria with the detergent TritonX100, indicating that it is located in the internal compartments of mitochondria (Figure 1D and E). During apoptosis, mitochondria undergo profound modifications (Cereghetti and Scorrano, 2006); therefore, we tested whether mitochondrial MDM4 is modified in this condition. No change in expression levels and localization of mitochondrial MDM4 (Figure 1E, right panel) could be detected on activation of apoptosis in MCF7 cells by a lethal dose of ultra-violet (UV) irradiation (Supplementary Figure S2). Under the same conditions, p53 relocalized at the mitochondria and was partly degraded, indicating that a fraction of it is in the internal compartments of mitochondria as well (Figure 1E, right panel).

To ascertain which region of MDM4 contributes to its mitochondrial localization, we expressed different MDM4 deletion mutants (Figure 2A) in *p53*$^{-/-}$*Mdm4*$^{-/-}$MEFs. All mutants, except MDM4-BD, were clearly recoverable with the mitochondria, suggesting that the COOH terminus mediates this localization (Figure 2B and C).

Overall, these results indicate that MDM4 is internally localized in the mitochondria, seemingly through its COOH terminus, and that its status does not change during the DNA-damage-induced apoptosis.

MDM4 facilitates p53-intrinsic apoptosis

The presence of MDM4 at mitochondria led us to hypothesize that MDM4 may affect p53-mediated mitochondrial apoptosis (also called p53-intrinsic apoptosis). Indeed, p53 activates the apoptosis through two distinct pathways: transcriptional activation of proapoptotic genes and facilitation of MOMP with release of cytochrome C (Chipuk and Green, 2006). Cytoplasmic localization of p53 is a prerequisite for the latter activity (Marchenko *et al*, 2000; Chipuk *et al*, 2004). Thus, we determined p53 localization on its co-expression with MDM4 in *p53*$^{-/-}$*Mdm4*$^{-/-}$MEFs. Western blot (Wb) analysis of cytoplasmic and nuclear fractions showed an increase in p53 levels, particularly in the cytoplasm (Figure 3A). Comparable results were obtained in MEFs from *p53*$^{-/-}$*Mdm2*$^{-/-}$ DKO mice (Figure 3B), indicating that this effect is independent of the presence of the p53-nucleoshuttling protein Mdm2. These data were further confirmed by quantification of coimmunofluorescence of *p53*$^{-/-}$*Mdm4*$^{-/-}$ MEFs (Figure 3C and D) and of *p53*$^{-/-}$*Mdm2*$^{-/-}$ MEFs (data not shown).

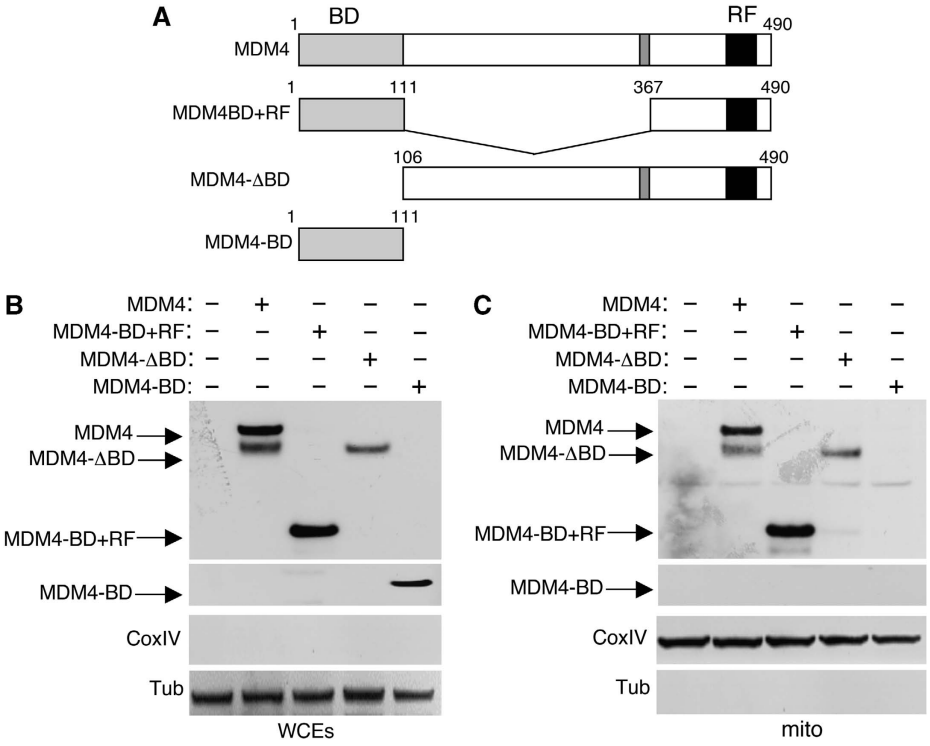

Figure 2 COOH terminus of MDM4 mediates its mitochondrial localization. (**A**) Scheme of MDM4 deletion mutants used in (B). BD is p53-binding domain, RF is Ring Finger domain. (**B**, **C**) Wb analysis of WCEs and mitochondrial fraction of *p53*$^{-/-}$*Mdm4*$^{-/-}$MEFs expressing the MDM4 deletion mutants depicted in (A).

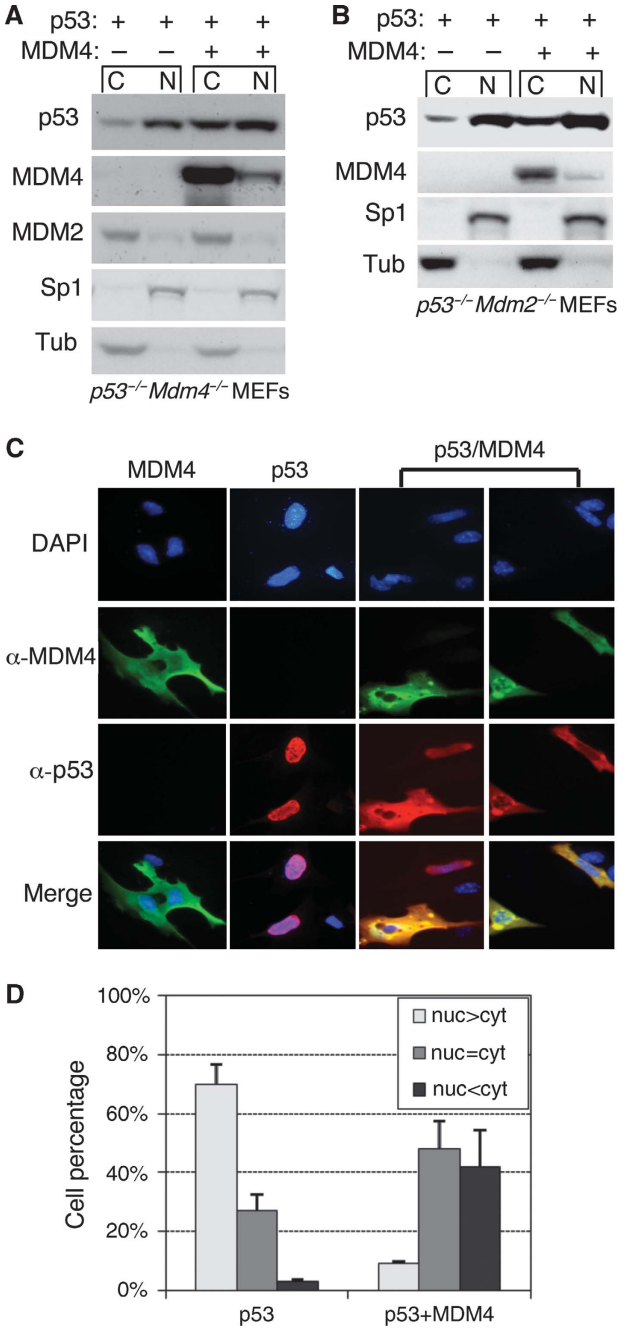

Figure 3 MDM4 increases p53 cytoplasmic levels more strongly than nuclear ones. (**A**) $p53^{-/-}Mdm4^{-/-}$MEFs were transiently transfected with indicated plasmids (molar plasmid ratio of p53:MDM4, 1:2) and nuclear and cytoplasmic fractions analysed by Wb. Cytoplasmic and nuclear contamination was verified by staining with α-tubulin and α-Sp1, respectively. (**B**) $p53^{-/-}Mdm2^{-/-}$ MEFs were transiently transfected with indicated proteins (p53:MDM4 molar plasmid ratio, 1:3) and cytoplasmic and nuclear fractions analysed by Wb. (**C**) $p53^{-/-}Mdm4^{-/-}$MEFs were transfected with indicated plasmids as in (A) and after 24 h, fixed and stained for MDM4 (green) and p53 (red). DNA (blue) is stained with DAPI. (**D**) p53-staining pattern was scored for 100 cells in two separate experiments. Each bar represents the mean and lines indicate standard deviation (s.d.). Cells were scored as having fluorescence stronger in the nucleus (nuc > cyt), equal in the nucleus and cytoplasm (nuc = cyt) or stronger in the cytoplasm (nuc < cyt).

Cytoplasmic p53 relocalizes to mitochondria only in response to apoptotic stimuli (Marchenko *et al*, 2000). However, overexpression of p53 can lead to its partial localization to these organelles (Dumont *et al*, 2003). We, therefore, analysed the cytosolic and mitochondrial fractions of p53 overexpressed in $p53^{-/-}Mdm4^{-/-}$MEFs in the presence or absence of MDM4. P53 was clearly detectable at the mitochondria in the presence of MDM4, but barely detectable in its absence (Figure 4A). In addition, MDM4 co-expression was associated with a significant release of cytochrome C, a hallmark of mitochondrial permeabilization, suggesting that the relocalized p53 was competent in driving intrinsic apoptosis. Indeed, the mitochondrial p53 was phosphorylated at Ser46, a modification associated with p53 proapototic activity (Oda *et al*, 2000; D'Orazi *et al*, 2002; Rinaldo *et al*, 2007) (Figure 4A). These data are in agreement with the report by Chipuk *et al*, who showed that cytosolic localization of p53 is sufficient to induce cytochrome C release and apoptosis independently of DNA damage in MEFs (Chipuk *et al*, 2004).

Overexpression of MDM4 causes increase of p53 levels (Jackson and Berberich, 2000; Stad *et al*, 2000) (Figure 4A). Thus, mitochondrial localization of p53 in the presence of MDM4 might merely depend on the MDM4-mediated increase of its cytoplasmic levels. To verify this possibility, we transfected different amounts of p53 to obtain approximately similar protein levels as those obtained by MDM4 co-expression. Higher expression of p53 resulted in its increased mitochondrial localization independently of MDM4 (Figure 4B). However, only in the presence of MDM4, there was (i) a specific increase of the proapoptotic p53Ser46^{P} form, whereas p53Ser15^{P} was unchanged, (ii) a significant release of cytochrome C (Figure 4B) and (iii) a specific increase of apoptotic, annexin-positive cells (Figure 4C). These data indicate that under these conditions, the mitochondrial localization of p53 depends on its cytoplasmic levels, whereas MDM4 specifically increases the proapoptotic p53Ser46^{P} form and the induction of apoptosis, suggesting that MDM4 promotes or facilitates p53-intrinsic apoptosis. Sole expression of MDM4 did not affect cell viability, suggesting the p53 dependency of its proapoptotic activity (Figure 4C). Co-expression of p53 and the MDM4 mutant unable to localize to the mitochondria (MDM4-BD) did not promote p53-dependent cell death (Figure 4D) and led to markedly reduced p53Ser46^{P} (Figure 4E), even though it enhanced p53 levels and mitochondrial localization as well as wild-type MDM4, suggesting that the mitochondrial localization of MDM4 might have an important role in its proapoptotic activity. In addition, an MDM4 mutant localized at the mitochondria, but unable to bind p53 (MDM4-ΔBD), neither promoted p53-dependent cell death (Figure 4D), nor induced p53Ser46^{P} comparable to wt-MDM4 (Figure 4F), suggesting that the proapoptotic activity of MDM4 requires its association with p53. Similar results were obtained in E1A/Ha-Ras(Val12) transformed $p53^{-/-}Mdm4^{-/-}$MEFs, a model prone to p53-mediated cell apoptosis (Supplementary Figure S3).

Taken together, these data confirm that MDM4 might act as a positive regulator of p53-intrinsic apoptosis.

Earlier studies on p53-intrinsic apoptosis have pointed to p53 ability to permeabilize membranes of isolated mitochondria and permit cytochrome C release (Mihara *et al*, 2003; Chipuk *et al*, 2004; Deng *et al*, 2006). Thus, we investigated

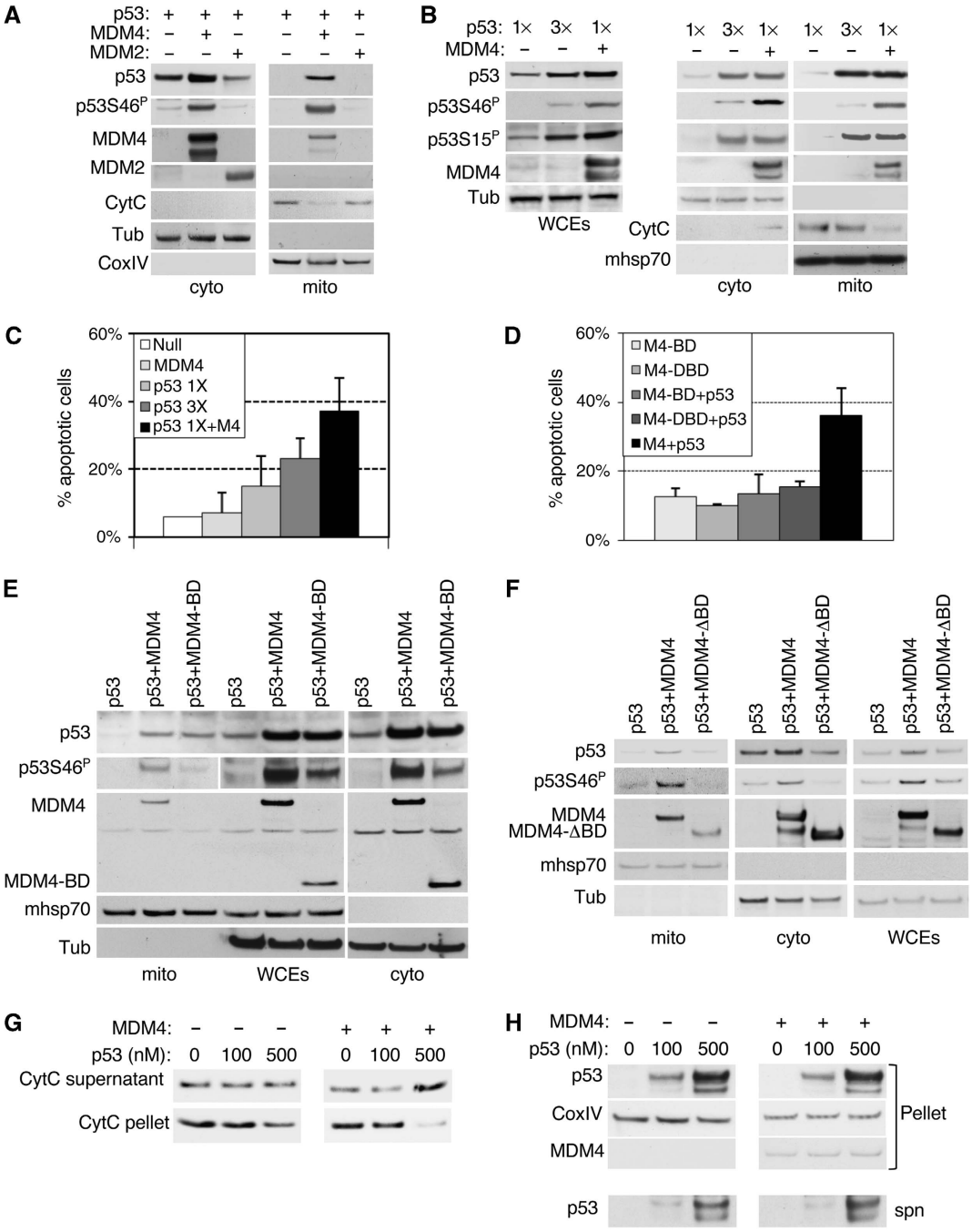

Figure 4 Mitochondrial MDM4 facilitates localization of proapoptotic p53Ser46^{P} at the mitochondria and p53-mediated release of cytochrome C. (**A**) *p53*$^{-/-}$*Mdm4*$^{-/-}$MEFs transfected with p53 and MDM4 or MDM2 (molar plasmid ratio of p53:MDM4 or MDM2, 1:2) were fractionated in cytosolic and mitochondrial preparations and analysed by Wb. (**B**) *P53*$^{-/-}$*Mdm4*$^{-/-}$MEFs were transfected with different amounts of p53: 0.5 μg of p53 (1 ×), 1.5 μg of p53 (3 ×) and 1 μg of MDM4. Mitochondrial and cytosolic fractions and WCEs were analysed by Wb. (**C**, **D**) *P53*$^{-/-}$*Mdm4*$^{-/-}$MEFs were transfected with indicated plasmid plus 1/5 of GFP. After 24 h, cells were stained with annexin-V and scored as percentage of GFP expressing cells. Each bar represents the mean and lines indicate standard deviation (s.d.). (**E**, **F**) WCEs and subcellular fractions of *p53*$^{-/-}$*Mdm4*$^{-/-}$MEFs transfected with p53 and MDM4, MDM4-BD (E) or MDM4-ΔBD (F) (molar plasmid ratio of p53:MDM4 variants, 1:2) were analysed by Wb. (**G**, **H**) Mitochondria isolated from *p53*$^{-/-}$*Mdm4*$^{-/-}$MEFs transfected with empty vector or MDM4 were reacted with indicated concentration of recombinant p53. After 60 min incubation at 37°C, reactions were centrifuged and pellet and supernatant (spn) fractions analysed by Wb.

whether MDM4 is required for p53-mediated MOMP in this cell-free system by testing the ability of recombinant p53 to permeabilize mitochondria isolated from *p53*$^{-/-}$*Mdm4*$^{-/-}$MEFs re-expressing MDM4 or a control vector (Figure 4G and H). Figure 4G shows that p53 caused weak release of cytochrome C from *p53*$^{-/-}$*Mdm4*$^{-/-}$ mitochondria. In comparison, the presence of mitochondrial MDM4 greatly enhanced such release resulting in depletion of cytochrome C from pellets and a corresponding increase in the supernatant. These data, confirmed by *in vitro* translated proteins (Supplementary Figure S4), strongly support the existence of a positive role of mitochondrial MDM4 in sustaining this p53 function.

MDM4 acts as a docking site for p53Ser46^{P} to BCL2

The cytochrome C release mediated by p53 depends on its ability to bind members of the antiapoptotic Bcl2 family (i.e. BCL2 and Bcl-xL) and to inactivate their inhibitory effect on the proapoptotic proteins Bax and Bak (Mihara *et al*, 2003; Deng *et al*, 2006). We, therefore, tested whether MDM4 affects p53 binding to BCL2. We co-expressed BCL2, p53 and MDM4 in *p53*$^{-/-}$*Mdm4*$^{-/-}$MEFs and analysed their immunocomplexes by Wb. Association between p53 and BCL2 was clearly evident in the presence of MDM4, but not in its absence (Figure 5A and B), suggesting that MDM4 greatly enhances this binding. Coimmunoprecipitation of *in vitro* translated proteins confirmed these data (data not shown). As MDM4 is present in the BCL2 immunocomplex (Figure 5B) and both proteins stably reside at the mitochondria, we asked whether MDM4 is bound to BCL2 or it co-precipitates with p53. Interestingly, we observed that MDM4 and BCL2 interact independently of the presence of p53 (Figure 5C and D). This binding was also observed between *in vitro* translated proteins, suggesting the existence of a direct interaction between MDM4 and BCL2 (Supplementary Figure S5A). Of relevance, this binding also occurs between endogenous mitochondrial proteins in normal growth conditions, as detected in mitochondria of MCF7 cells, dependent on the MDM4 levels (Figure 5E). This association was not altered by a lethal dose of UV (Figure 5F), whereas p53 binds MDM4 at the mitochondria only on induction of apoptosis (Figure 5F), suggesting that MDM4 may act as a docking site for p53 binding to BCL2 under these conditions. Indeed, the expression of a mutant MDM4 unable to bind p53 (MDM4-ΔBD) does not promote the association of p53 with BCL2 (Supplementary Figure S5B). Most importantly, the association of endogenous mitochondrial p53 with BCL2 is strongly impaired after reduction of MDM4 levels (Figure 5G), supporting the model of MDM4 as a mitochondrial anchor for p53/BCL2 association.

As MDM4 expression preferentially caused mitochondrial localization of p53Ser46^{P}, we tested whether this specific

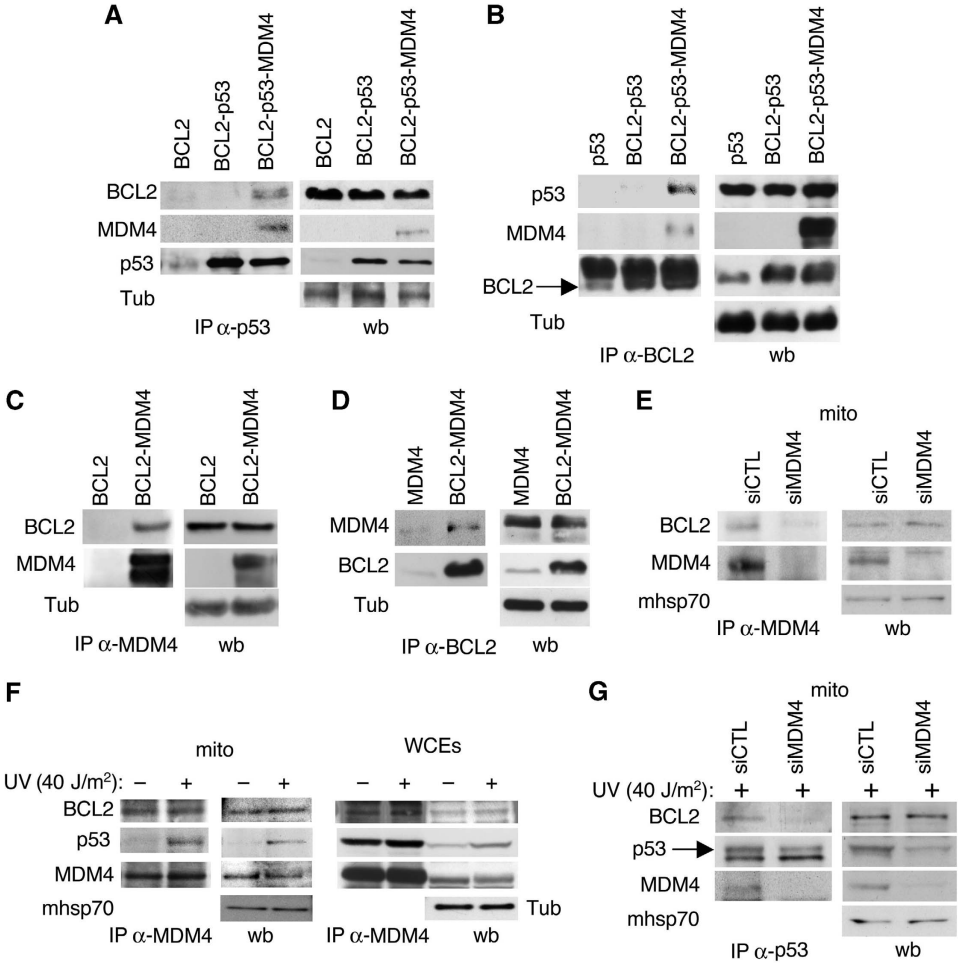

Figure 5 MDM4 binds BCL2 and facilitates binding between mitochondrial p53 and BCL2. (**A**, **B**) *p53*$^{-/-}$*Mdm4*$^{-/-}$MEFs were transfected with indicated plasmids (molar plasmid ratio of p53:BCL2, 1:2; P53:BCL2:MDM4 0.5:2:1) and p53 and BCL2 immunocomplexes analysed after immunoprecipitation of 600 μg of WCE with α-p53, FL393 (A) or α-BCL2, C2 antibodies (B). Wb indicates analysis of 1/10 of WCEs. (**C**, **D**) *p53*$^{-/-}$*Mdm4*$^{-/-}$MEFs were transfected with equimolar amounts of the indicated plasmids and MDM4 and BCL2 immunocomplexes analysed after immunoprecipitation of 600 μg of WCE with α-MDM4, BL-1258 (C) or α-BCL2, C2 antibodies (D). (**E**) Analysis of MDM4 immunocomplexes in mitochondria of MCF7 cells transfected with siCTL or siMDM4. 100 μg of mitochondrial lysates were immunoprecipitated with α-MDM4, BL1258 and proteins present in the immunocomplex analysed by Wb. (**F**) Analysis of MDM4 immunocomplexes in MCF7 cells either untreated or treated with UV 40 J/m^2. After 3 h from UV, 2 mg of WCEs or 100 μg of mitochondrial lysates were immunoprecipitated with α-MDM4, BL1258 and proteins present in the immunocomplex analysed by Wb. (**G**) Analysis of p53 immunocomplexes in MCF7 cells transfected with siCTL or siMDM4 and treated with UV 40 J/m^2. After 7 h, 200 μg of mitochondrial lysates were immunoprecipitated with α-p53, PAb-421 and proteins present in the immunocomplex analysed by Wb.

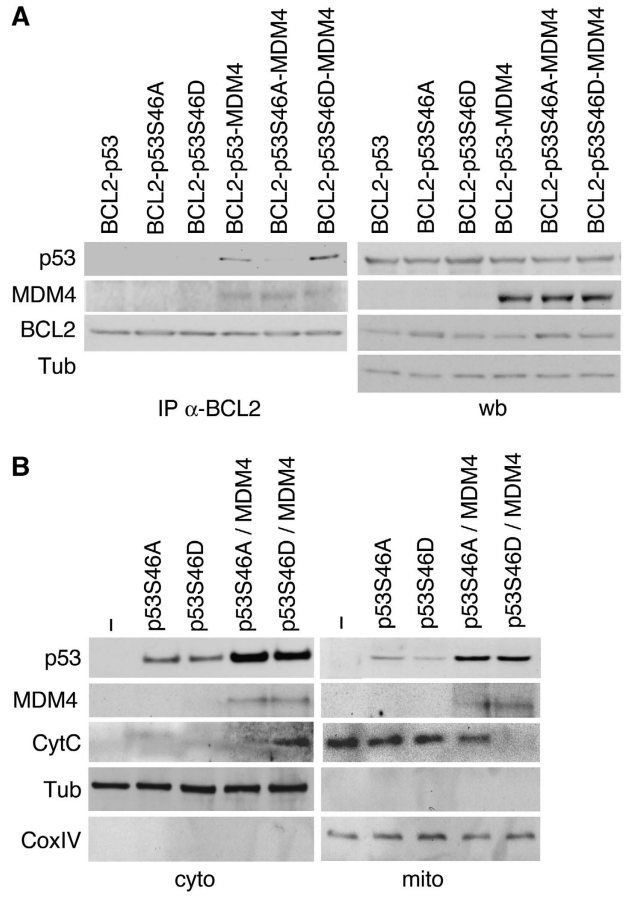

Figure 6 In the presence of MDM4, BCL2 binds p53Ser46^{P} preferentially. (**A**) *p53*$^{-/-}$*Mdm4*$^{-/-}$MEFs were transfected with p53, p53S46D or p53S46A and BCL2, and MDM4 (molar plasmid ratio of p53:BCL2, 1:2; P53:BCL2:MDM4 0.5:2:1), and BCL2 immunocomplexes analysed after immunoprecipitation of 600 μg of WCE with α-BCL2, C2 antibody. (**B**) Wb of cytosolic and mitochondrial fractions of *p53*$^{-/-}$*Mdm4*$^{-/-}$MEFs transfected with the indicated plasmids (molar plasmid ratio of p53:MDM4, 1:2).

modification affects p53 binding to BCL2. In the absence of MDM4, neither the P53S46D, that mimics the phosphorylated p53Ser46^{P} (Mayo *et al*, 2005), nor the p53S46A, that mimics the absence of Ser46 phosphorylation, associated with BCL2. On the contrary, in the presence of MDM4, the mutant p53S46D associated with BCL2 nearly as much as wt-p53, whereas the mutant p53S46A was barely associated (Figure 6A). These data indicate that the Ser46 phosphorylation is necessary, but not sufficient to induce p53/BCL2 association and confirm the requirement of MDM4 to promote this association. In agreement with the low BCL2 binding, p53S46A co-expressed with MDM4-induced weak release of cytochrome C (Figure 6B). In contrast, p53S46D promoted an almost complete release of cytochrome C from mitochondria (Figure 6B). Taken together, these data indicate that MDM4 facilitates the association between BCL2 and p53Ser46^{P} proteins, favouring the mitochondrial-apoptotic activity of the latter.

Endogenous MDM4 facilitates p53-mediated intrinsic apoptosis

To verify whether the mitochondrial MDM4 activity described above reflects an *in vivo* function, endogenous MDM4 was decreased by small interfering RNA (siRNA) in MCF7 cells and cell survival measured under different stressing conditions. Whole cell extracts (WCEs) of MCF7 cells exposed to sublethal or lethal doses of UV (2 and 40 J/m^2, respectively) (Supplementary Figure S2) were fractionated in mitochondria and cytosol and analysed by Wb. On sublethal dose, MDM4 levels decreased according to what was described earlier (Kawai *et al*, 2003; Pan and Chen, 2003; Pereg *et al*, 2005). On the contrary, after a lethal dose of irradiation, MDM4 levels were similar to CTL, whereas MDM2 levels were almost undetectable (Figure 7A). Only on lethal dose, p53 and its Ser46 phosphorylated form were detectable both in the cytoplasm and at the mitochondria associated with cytochrome C release (Figure 7A). Under comparable stressing conditions, MDM4 interference did not substantially alter cytosolic levels of p53 and p53Ser46^{P} (Figure 7B), but induced a marked decrease of total p53 and, to a greater extent, of p53Ser46^{P} in the mitochondrial fraction (Figure 7C). Noteworthy, this phenomenon correlated with the retention of cytochrome C in the mitochondria, indicating that MOMP is partially impaired by MDM4 reduction (Figures 7B and C). In agreement with these data, cell death analyses showed decreased apoptosis of the MDM4-interfered cells (Figure 7D, upper panel). Particularly, analysis of mitochondrial potential showed an increased resistance of MDM4-interfered cells to the collapse of the electrochemical gradient across the mitochondrial membrane supporting a positive role for MDM4 in mitochondrial-intrinsic apoptosis (Figure 7D, lower panel). Similar MDM4 activity was also observed in p53$^{+/+}$HCT116 cells after lethal adriamycin (Adr) treatment or UV irradiation (Supplementary Figure S6A, C, E and F) (Rinaldo *et al*, 2007). Notheworthy, p53-null HCT116 cells (p53$^{-/-}$HCT116) did not exhibit significant modification of cell survival under the same conditions (Supplementary Figure S6B and D), confirming the role of p53 in MDM4-proapoptotic activity.

MDM4 binds to p53 and inhibits its transcriptional activity. Thus, MDM4 depletion might alter transcriptional pathways that, in turn, might impinge on mitochondrial function and inhibit apoptosis through mechanisms independent of the MDM4/p53 mitochondrial localization. To evaluate this possibility, we performed experiments similar to those reported in Figure 7A–D under transcriptional blockade by using α-amanitin, a specific inhibitor of polymerase II-dependent transcription and an activator of p53-mitochondrial apoptosis (Arima *et al*, 2005) (Figure 7E). In the presence of α-amanitin, decrease of MDM4 was still able to reduce the levels of p53, and especially of p53Ser46^{P}, at the mitochondria with concurring retention of cytochrome C (Figure 7F) and increased cell survival (Figure 7G). These results confirm the transcription-independent activity of MDM4 in induction of apoptosis and further support its positive regulation towards p53-intrinsic apoptosis.

MDM4 expression correlates with tumour sensitivity to cisplatin

Although the relevance of p53-intrinsic apoptosis in the global p53 response to chemotherapy has not yet been quantified (Erster and Moll, 2005), it has been reported that mitochondrial accumulation of p53 and caspase-dependent mitochondrial apoptosis are specifically disrupted in ovarian cancer cells resistant to cisplatin treatment (Yang *et al*, 2006).

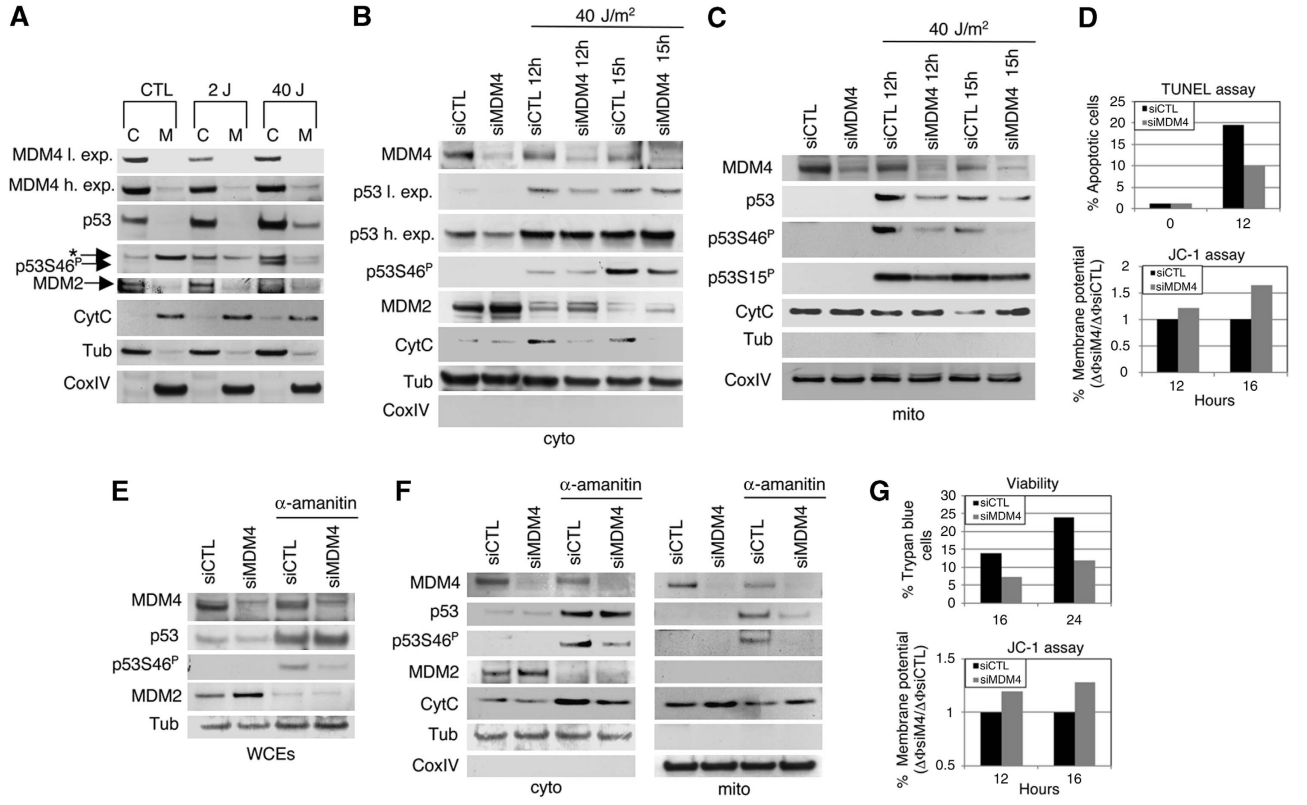

Figure 7 MDM4 depletion decreases mitochondrial permeabilization and cell death of MCF7 cells, independently of transcription. (**A**) Wb analysis of cytosolic and mitochondrial fractions of MCF7 collected 8 h after irradiation with a sublethal (2 J/m^2) or lethal dose (40 J/m^2) of UV. *Indicates an unspecific band. L, h and exp indicate low and high exposure, respectively. (**B–D**) MCF7 cells were transfected with siCTL or siMDM4 (30 nM) and after 24 h cells were either untreated or treated with 40 J/m^2. At the indicated time points, cytosolic (B) and mitochondrial (C) fractions were collected and analysed by Wb. (D) Apoptosis was assessed by counting the number of TUNEL-positive cells (upper panel) or analysis of mitochondrial membrane potential by JC-1 staining (ΔΦ) (lower panel). Data are shown as per cent of increase of membrane potential of siMDM4 cells to siCTL cells at the indicated time points. The ratio (ΔΦsiM4/ΔΦsiCTL) was calculated after normalization of each ΔΦ to that of the corresponding untreated cells. The data are representative of three independent experiments. (**E–G**) MCF7 cells were transfected with siCTL or siMDM4 and after 24 h either untreated or treated with 10 μg/ml α-amanitin. After 16 h, WCEs (E), cytosolic and mitochondrial (F) fractions were collected and analysed by Wb. (G) Cell death was assessed by counting the number of cells positive to Trypan blue staining (upper panel) or by JC-1 assay as described earlier (D).

We, therefore, investigated whether MDM4 is involved in drug sensitivity of the wild-type *TP53*-carrying A2780 ovarian cancer cells in comparison to their derivative, the cisplatin-resistant wild-type *TP53*-carrying A2780cis cells (Behrens *et al*, 1987). Interestingly, p53 protein levels were comparable in the two populations, whereas MDM4 levels were strongly downregulated in A2780cis cells (Figure 8A). In parental A2780 cells, MDM4 reduction significantly decreased the levels of mitochondrial p53Ser46^P, without affecting the total amount of p53 (Figure 8B and C), and cell susceptibility to cisplatin, as shown by apoptotic assays (Figure 8D–F). Analysis by real-time polymerase chain reaction (RT–PCR) of p53-transcriptional targets (NOXA and p21) indicated that siMDM4 did not alter the mRNA levels of these genes up to 16 h, confirming the transcription-independent proapoptotic activity of MDM4 (data not shown). Conversely, in drug-resistant A2780cis cells, overexpression of MDM4 increased both cell susceptibility to cisplatin and levels of p53Ser46^P (Supplementary Figure S7).

To evaluate whether the relationship between apoptotic function of MDM4/p53 and cisplatin susceptibility defined in A2780 cells occurs *in vivo*, we analysed the mRNA levels of full-length *MDM4* and its oncogenic *MDM4-S* variant (Rallapalli *et al*, 1999) in a group of 17 wild-type *TP53*-carrying ovarian tumour samples and correlated these levels with the cisplatin responsiveness of the patients (Supplementary Table 1). A significant correlation between fl-MDM4, but not MDM4-S, expression and patients' response to the drug was found (Figure 8G). In particular, tumours characterized by higher levels of *MDM4*, confirmed at the protein levels (Figure 8H and I), showed complete remission after chemotherapy in comparison to those expressing lower levels of MDM4, supporting the existence of an MDM4-dependent modulation of drug susceptibility in human tumours, similarly to the results we obtained with the A2780 cancer cells.

Discussion

The present study describes a new localization for MDM4 at the mitochondria in which it binds BCL2, and provides evidence that MDM4 acts as a mitochondrial anchor for p53Ser46^P and facilitates p53-intrinsic-apoptotic pathway.

The MDM4 localization at the mitochondria is stable one, is unaffected by genotoxic stress (Figure 1) and is seemingly mediated by the MDM4 COOH terminus where the Ring

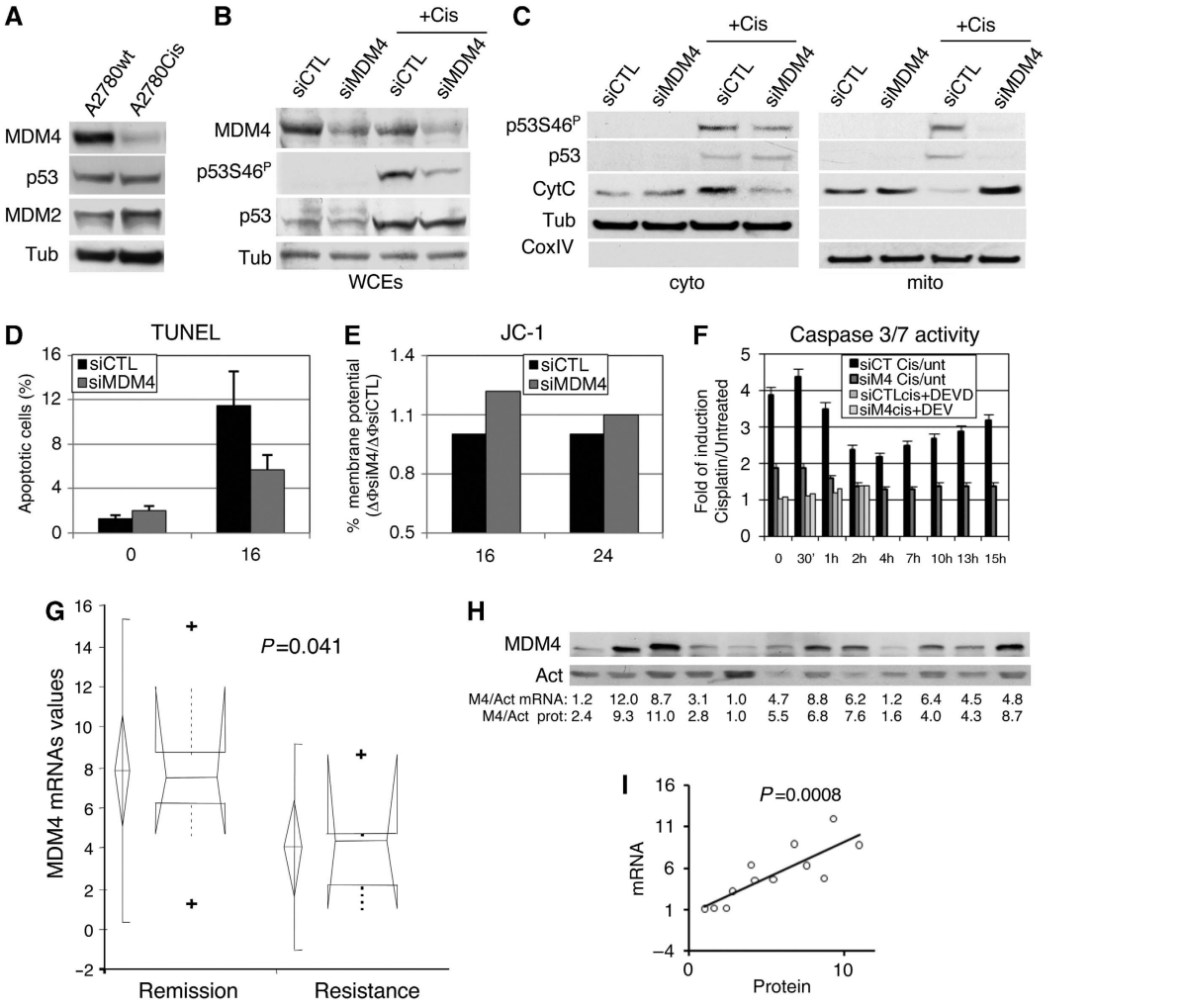

Figure 8 MDM4 levels correlate to and modulate cisplatin sensitivity. (**A**) Wb analysis of WCEs of A2780 and ciplatin resistant, A2780Cis cells. (**B**, **C**) Wb analysis of WCEs (B) or cytosolic and mitochondrial fractions (C) of A2780 cells transfected with siCTL or siMDM4 (30 nM) and after 24 h treated or untreated with cisplatin 20 μM for 20 h. (**D**–**F**) Cells were treated as in (B) and at the indicated time points, apoptosis was analysed by TUNEL assay (D), JC-1 assay (E) or caspase 3/7 activity (F). JC-1 assay was performed as described earlier (Figure 7D). Caspase 3/7 activity was analysed after 16 h of cisplatin treatment by measurements of a caspase 3/7 canonical fluorescence substrate (Z-DEVD-R110) at the indicated time points. At each time point, one sample was treated with caspase inhibitor DEVD. Values show the ratio of caspase 3/7 activity of treated to untreated cells. Each bar represents the mean of eight measures. (**G**) Comparison of *MDM4* mRNA levels between samples of ovarian cancer grouped in resistance or remission (see Supplementary Informations for definition). Each plot shows graphically the central location and scatter/dispersion of the values of each group: the line series shows parametric statistics (mean and confidence interval of mean), whereas the notched box and whiskers show non-parametric statistics (median, confidence interval of median and inter-quartile range). Crosses indicate possible outliers between 1.5 and 3 inter-quartile range. *P*-value was calculated according to independent samples *t*-test ($n = 17$ $t = -2239$). (**H**) Wb analysis for the indicated proteins of WCEs of 12 out of 17 tumour samples analysed in G. The values derive from the ratio of densitometric values of MDM4 to actin, both at the protein and mRNA levels. (**I**) Linear regression between MDM4 corrected protein and mRNA levels. *P*-value was calculated according to Linear regression test.

Finger (RF) domain is located (Figure 2). These data are in agreement with observations by Migliorini *et al*, who showed that deletion of the MDM4 C-terminal domain causes re-distribution of the MDM4 protein to the nucleus and its decreased presence in the cytoplasm (Migliorini *et al*, 2002b). Our data suggest that mitochondrial MDM4 is not associated with MDM2. Indeed, we never observed the latter protein at the mitochondria. As MDM2 interacts with MDM4 through the RF domain (Sharp *et al*, 1999; Tanimura *et al*, 1999), the engagement of this domain in the association of MDM4 with the mitochondria might prevent MDM2 binding.

Our data are compatible with mitochondrial MDM4 being located in the internal compartments of these organelles. Indeed, MDM4 is protected from enzyme degradation (Figure 1D and E). Its binding to BCL2 (Figure 5), which is tail anchored to the outer mitochondrial membrane, suggests that MDM4 is located in the outer membrane. Mitochondrial MDM4 does not apparently function as an anchor for BCL2 as its depletion does not alter the presence of BCL2 at the mitochondria (Figure 5E and G). In contrast to this, MDM4 binds to and relocalizes p53 at the mitochondria. It remains to ascertain whether MDM4 contacts the enzyme-protected mitochondrial fraction of p53 or the p53 fraction externally associated with the mitochondria, similarly to the association of p53 with the integral mitochondrial protein Bak (Leu *et al*, 2004).

Although overexpression experiments indicate that p53 relocalization at the mitochondria mainly correlates with the total p53 levels, reduction of endogenous MDM4 causes a specific decrease of levels of mitochondrial p53 and parti-

cularly of the p53Ser46^{P} (Figure 7), suggesting that MDM4 may function as an anchor for this phosphorylated form at BCL2. Indeed, association of p53S46D with BCL2 is strongly enhanced by the presence of MDM4 (Figure 6A). As our data indicate that unmodified MDM4 binds with similar affinity unphosphorylated and phosphorylated p53Ser46 (data not shown), it may be hypothesized that the selectivity towards the p53Ser46^{P} form resides in the MDM4/Bcl2 complex. It remains to ascertain whether MDM4 directly modifies the levels of this phosphorylated protein or the mitochondrial association of p53Ser46^{P} with BCL2 affects its stability.

Overall, our data support a role for mitochondrial MDM4 fraction in sustaining its proapoptotic function. Indeed, the requirement of physical interaction between MDM4 and p53 to promote p53/BCL2 association (Supplementary Figure 5B), and of the MDM4 presence for the association of endogenous mitochondrial p53 with BCL2, confirms this hypothesis. In addition, experiments with isolated mitochondria re-expressing MDM4 (Figure 4G and H) support the role of mitochondrial MDM4 in promoting p53-mediated intrinsic apoptosis.

Our data further indicate that p53Ser46^{P} is a preferential partner for BCL2 and a more active form in promoting p53-intrinsic apoptosis (Figure 6A and B). Thus far, analysis of post-translational modifications of mitochondrial p53 has shown the presence of p53Ser46^{P} at this subcellular site (Nemajerova *et al*, 2005). However, the ability of different p53 modifications to mediate the intrinsic-apoptotic pathway has not been tested. Interestingly, the mitochondrial protein WOX1, a WW domain-containing oxidoreductase, was shown to selectively bind p53Ser46^{P}, conferring cell sensitivity to apoptotic stress (Chang *et al*, 2005). In addition, Feng *et al* reported a significant decrease of thymocite apoptosis in transgenic mice carrying the human mutant p53S46A (Feng *et al*, 2006). As thymus is a tissue in which p53 exerts an important mitochondrial function (Moll *et al*, 2005), these data support a role of p53Ser46^{P} in mitochondrial apoptosis.

Overall, our data indicate a positive activity exerted by MDM4 towards p53-intrinsic apoptosis. This finding apparently contradicts two properties so far known for MDM4: (i) a negative regulation of p53 and (ii) its inactivation during the stress response aimed to release p53 activity (Marine *et al*, 2006, 2007; Toledo and Wahl, 2006). Although different models have been proposed to explain the negative regulation exerted by MDM4 towards p53, they generally apply to regulation under basal or sublethal conditions. Indeed, the antagonistic function of MDM4 towards cell viability concurs often with highly increased levels of MDM2 and p21, events resembling a growth arrest response (Gilkes *et al*, 2006). On the contrary, the data here reported refer to a function of MDM4 under lethal genotoxic stress, particularly in the p53-intrinsic-apoptotic pathway. In this respect, they are in agreement with the positive effect of overexpressed MDM4 towards p53-mediated apoptosis (Mancini *et al*, 2004). They might also be considered consistent with the strong apoptotic response observed in *Mdm2*-KO mice (Chavez-Reyes *et al*, 2003). Indeed, although the relevance *in vivo* of p53-intrinsic apoptosis in the general apoptotic process has not been quantified, cell death in *Mdm2*-KO mice might be also caused by the persistence or even the increase of mitochondrial MDM4 and by its ability to promote p53-mitochondrial apoptosis. Of note, MDM4 levels are higher in the thymus, a tissue in which p53 exerts an important mitochondrial function (Shvarts *et al*, 1997; Moll *et al*, 2005).

With respect to the inactivation of MDM4 occurring during the stress responses, this has been tightly associated with the activation of the degradative activity of MDM2 (Marine *et al*, 2007). However, various evidences suggest distinct activities of MDM2 under different stress conditions. Indeed, on a sublethal type of damage usually associated with a growth arrest, MDM2 levels are strongly increased. On the contrary, on a lethal damage leading to an apoptotic outcome, MDM2 levels do not increase or even decline (Ashcroft *et al*, 2000; Latonen *et al*, 2001; Meng *et al*, 2007; Rinaldo *et al*, 2007). Destabilization of the MDM2 protein caused by increased autodegradation after DNA damage has also been described, although the type of cell response associated with it has not been established (Stommel and Wahl, 2004; Tang *et al*, 2006). Finally, impairment of MDM2-degradative activity towards specific proapoptotic targets has also been suggested. Marchenko *et al* have shown a decrease of MDM2-mediated polyubiquitylation of p53 during the apoptosis (Marchenko *et al*, 2007). In agreement with all these data, a recent model considers the upregulation of MDM2 during the growth arrest, an event favouring this cell response in respect to cell death (Shmueli and Oren, 2007). In agreement with this model, we observe a strong decrease of MDM2 expression in MCF7 cells after a lethal dose of UV (Figure 7A).

MDM4 degradation is also associated with its nuclear translocation and binding to 14-3-3 proteins (Jin *et al*, 2006; LeBron *et al*, 2006; Pereg *et al*, 2006). In view of a role of MDM4 in the intrinsic apoptosis, an additional interpretation for these observations may be also provided. Both these events may sequester MDM4 from the cytoplasmic pool and consequently from the mitochondrial site, thus preventing p53-proapoptotic activation when cell cycle arrest is required. In fact, 14-3-3 proteins are crucial apoptosis inhibitors that exert their function by binding and inactivating proapoptotic proteins involved in the mitochondrial pathway (Porter *et al*, 2006).

Noteworthy, our findings indicate that MDM4-proapoptotic activity may have an *in vivo* relevance by affecting cell susceptibility to DNA-damage induced by cisplatin. Although these data need a confirmation in a large population study, their implication in predicting cancer response to therapy seems relevant.

Finally, the integration of MDM4 inhibition of cell cycle arrest with its proapoptotic function reported here supports and extends to MDM4 the new current model, based on the view of MDM2 as a p53 lifesaver (Rinaldo *et al*, 2007; Shmueli and Oren, 2007), that points to p53 regulators as not only controllers of p53 activity but also important players in the p53-mediated decision between cell life and death.

Materials and methods

Cell culture and transfections

The *p53*$^{-/-}$*Mdm2*$^{-/-}$MEF and *p53*$^{-/-}$*Mdm4*$^{-/-}$MEF (kindly provided by Dr G Lozano and Dr JC Marine, respectively), derived from KO mice, were cultured in DMEM high glucose supplemented with

10% FBS (Cambrex). All experiments were done between passage 4 and 8. E1A/Ha-Ras(Val12)-*p53*$^{-/-}$*Mdm4*$^{-/-}$MEFs were generated by puromycin selection of transfectants with the E1A and Ha-Ras (Val12) plasmids. E1A/Ras-*p53*$^{-/-}$*Mdm4*$^{-/-}$MEFs, MCF7, HCT116 and RKO cells were cultured in DMEM supplemented with 10% FBS (Invitrogen). A2780 and A2780cis cells were cultured in RPMI supplemented with 10% FBS (Invitrogen). Transient transfections in *p53*$^{-/-}$*Mdm2*$^{-/-}$MEFs, *p53*$^{-/-}$*Mdm4*$^{-/-}$MEFs and A2780cis cells were performed using Lipofectamine 2000 and in E1A/Ha-Ras(-Val12)-*p53*$^{-/-}$*Mdm2*$^{-/-}$MEFs using Lipofectamine Plus according to manufacturer's instructions (Invitrogen). MCF7 cells were treated with 10 μg/ml α-amanitin. Both A2780 and A2780cis cells were treated with cisplatin 20 μM, HCT116 cells were treated with Adr 1.8 μM. Plasmids used were pShuttle-hMdm4, pCDNA3.1-hMdm4, pCDNA3.1-hMdm4-BD + RF, pCDNA3.1-hMdm4-BD, pCDNA3.1-hMdm4-ΔBD, pCAG-hp53 (WT, S46A, S46D), pCMV-hMdm2 and pef-hBcl2. MDM4 deletion mutants were obtained by PCR amplification of fragments of the human *Mdm4* cDNA in the presence of specific pair of primers (available on request). Each construct contains the same Kozak consensus sequence flanking the first ATG. PCR products were cloned in the pcDNA3.1/mycHis(−) B (Invitrogen). All the constructs were analysed by DNA sequencing. MDM4-ΔBD contains aa residues from 106 to 489 (with a methionine upstream of aa 106). MDM4-BD contains the first 111 aa of MDM4. MDM4-BD + RF contains an internal deletion from aa 112 to 366.

Immunofluorescence

For mitochondrial staining, MCF7 cells were incubated with prewarmed (37°C) growth medium-containing MitoTracker Red CMXRos (Molecular Probes, Invitrogen) for 30 min. Cells were then fixed with 3.7% formaldehyde for 15 min at 37°C, permeabilized with 80% acetone in PBS and blocked with 5% bovine serum albumin (BSA). Cells were incubated with mouse α-MDM4 monoclonal antibody 6B1A and then incubated with Cy2-conjugated (green) affiniPure Donkey anti-mouse IgG (Jackson ImmunoResearch). DNA was stained with DAPI. Fluorescent cells were examined under a confocal laser scanning microscope (Leica SP5, Leica Microsystems) equipped with three laser lines: violet diode emitting at 405 nm, argon emitting at 488 nm and helium/neon emitting at 543 nm. Images were exported in JPEG, contrast and brightness were adjusted in Adobe Photoshop 7 and final figures were generated with Adobe Illustrator 10. For MDM4 and p53 coimmunofluorescence, *p53*$^{-/-}$*Mdm4*$^{-/-}$MEFs cells were fixed with 2% formaldehyde, permeabilized with TritonX100 0.25% and blocked with 5% calf serum. Cells were stained with Hoechst and primary antibodies: monoclonal α-Mdm4 antibody 6B1A and polyclonal α-p53 antibody Ab7. FITC- and Cy3-conjugated secondary antibodies were used. Cells were examined using a standard immunofluorescence microscope.

Adenoviruses generation and infection

The strategy to create recombinant adenovirus was as described earlier by Mancini *et al*. The fragment of cDNA coding for human MDM4 (nt 115–1629 according to BC067299 accession number) was cloned into the pAdShuttle-CMV vector (Stratagene). Adenoviral infections were carried out on cell monolayers (in 60 mm Petri dishes) at the indicated multiplicity of infections (MOIs) by 1 h incubation at 37°C in the presence of 1 ml of medium. Fresh culture medium was then added and cells were subjected to the treatments as indicated in the text.

Viability, apoptosis and caspase detection

Cell proliferation rate was assessed by determining cell number in a Thomas's haemocytometer, using Trypan blue exclusion test. Apoptosis was monitored by annexin V binding, measuring the mitochondrial membrane potential (ΔΦ), determining the activation of caspase 3 and detection of TUNEL positivity. Cells were harvested, pooled with the supernatant, washed once in PBS with Ca/Mg and processed for the different assays. Annexin assay (Clontech) was performed according to the manufacturer's instructions. For the measurement of the ΔΦ, the JC-1 staining was used. After washing in PBS with Ca/Mg, cells were resuspended in complete medium and incubated with 2.5 μg/ml JC-1 (Molecular Probes) for 20 min at room temperature in the dark. After two washes in PBS with Ca/Mg, samples were placed on ice and immediately analysed by a BD FACScan cytofluorimeter by using the BD CellQuest software package. As control, we used a sample treated with the depolarizing agent valinomicin for further 15 min before JC-1 staining. For TUNEL assay, cells were fixed in paraformaldehyde solution (4% in PBS, pH 7.4) for 30 min at room temperature and permeabilized with 0.1% TritonX100 in 0.1% sodium citrate for 2 min on ice. Apoptotic nuclei were detected using TUNEL labelling reaction according to the manufacturer's instructions (Roche Biochemicals). TUNEL labelling and phase contrast images were analysed by AXIO VISION 3.0 program. Caspase-3/7 assay (Promega) was analysed according to the manufacturer's instructions using Apo-ONE Homogeneous

Immunoprecipitation and Wb analysis

For immunoprecipitation experiments, cells were lysed in Saito's modified buffer (50 mM Tris–HCl, pH 7.4, 0.15 M NaCl, 0.5% Triton-X100, 5 mM EDTA). For binding between *in vitro* translated proteins (WGE, Promega), 20 μl of the 50-μl reaction were resuspended in 500 μl of Saito's modified buffer. Alternatively, for immunoprecipitation of p53 and detection of BCL2 and MDM4 EBC's modified buffer (50 mM Tris–HCl, pH 7.4, 0.12 M NaCl, 0.4% NP-40, 1 mM EDTA, 1 mM β-mercaptoethanol) was used. All buffers contained a cocktail of protease inhibitors (Boehringer). Immunoprecipitations were performed by preincubation lysates with protein G-sepharose (Pierce) and then with the indicated antibody, under gentle rocking at 4°C overnight. For Wb, cells were lysed in RIPA buffer (50 mM Tris–Cl, pH 7.5, 150 mM NaCl, 1% Nonidet P-40, 0.5% Na desoxicholate, 0.1% SDS, 1 mM EDTA) supplemented with a cocktail of protease inhibitors (Boehringer). All SDS–PAGE were transferred onto PVDF membranes (Millipore). Membranes were developed using the enhanced chemiluminescence (ECL Amersham). The following primary antibody were used: rabbit anti-MDM4 polyclonal antibody BL1258 (Bethyl laboratory), mouse anti-MDM4 monoclonal antibody 6B1A, mouse anti-MDM4 monoclonal antibody C82 (Sigma), mouse anti-BCL2 monoclonal antibody C2 (Santa Cruz), mouse anti-His Tag 4D11 (Upstate), mouse anti-c-myc monoclonal antibody 9E10 (Pharmingen), rabbit anti-BCL2 polyclonal antibody (N19 Santa Cruz Biotechnology), rabbit anti-p53 polyclonal antibody FL393 (Santa Cruz), sheep anti-p53 polyclonal antibody Ab7 (Oncogene Science), rabbit anti-p53S46^{P} and anti-p53S15^{P} polyclonal antibodies (Cell Signaling), mouse anti-p53 monoclonal antibody Ab1 (Calbiochem), mouse anti-MDM2 monoclonal antibody 2A10, mouse anti-α-tubulin monoclonal antibody DM1A (Sigma), mouse anti-mHsp70 monoclonal antibody JG1 (Affinity Bioreagent), mouse anti-Cytochrome C monoclonal antibody 7H8 (Santa Cruz), mouse anti-CoxIV monoclonal antibody 1D6 (Molecular Probes-Invitrogen), mouse anti-actin monoclonal antibody C-40 (Sigma) and rabbit anti-Sp1 polyclonal antibody PEP2 (Santa Cruz).

Isolation of nuclear/cytoplasmic fractions

Nuclear and cytoplasmic fractions were prepared as follows: $1–2 \times 10^6$ cells, scraped off the plate with PBS, were resuspended in hypotonic lysis buffer (10 mM HEPES pH 7.9, 10 mM KCl, 0.1 mM EDTA, 0.1 mM EGTA) added with protease inhibitors (Boehringer). After resuspension, NP-40 was added to a final concentration of 0.6% and the nuclei was isolated by centrifugation at 10 000 r.p.m. for 30 s at 4°C. After removal of the supernatant (i.e. the cytoplasmic extract), nuclei were resuspended in nuclear extract buffer (20 mM HEPES pH 7.9, 25% glycerol, 0.4 M NaCl, 0.1 mM EDTA, 0.1 mM EGTA), rocked for 15 min at 4°C and then recovered by centrifugation at 14 000 r.p.m. for 5 min at 4°C.

Isolation of mitochondria and treatment with proteinase K in vitro

Mitochondria were isolated by differential centrifugation, using Mitochondria Fractionation Kit (IMGENEX). For enzymatic digestion, isolated mitochondria were resuspended in suspension buffer and treated with proteinase K 0.2 mg/ml for MCF7 cells and 0.01 mg/ml for *p53*$^{-/-}$*Mdm4*$^{-/-}$MEFs cells for 20 min at 30°C in the presence or absence of TritonX100 (1% final concentration). Phenylmethylsulfonyl fluoride was then added to a final concentration of 2 mM to stop the reaction.

Cytochrome C release from isolated, purified mitochondria

Intact mitochondria were isolated as described earlier from MDM4^{+} DKO-MEFs or CTR-transfected *p53*$^{-/-}$*Mdm4*$^{-/-}$MEFs and incubated at 37°C for 1 h with increasing concentrations of

recombinant p53 (BD Pharmingen) in MSB buffer (400 mM mannitol, 50 mM Tris, pH 7.2, 10 mM KH_2PO_4, 5 mg/ml BSA) containing a cocktail of protease inhibitors. Samples were centrifuged at 5500 r.p.m. for 15 min. The resulting supernatant and pelleted mitochondrial fractions were analysed by Wb. Pelleted mitochondria were washed two times with MSB buffer before analysis. Alternatively, mitochondria isolated from $p53^{-/-}Mdm4^{-/-}$ MEFs were incubated with *in vitro* translated MDM4 and p53 proteins.

Small interfering RNA

MDM4 siRNA and control siRNA were generated by Invitrogen (Stealth RNAi) and consisted a mix of three different siRNA. Cells were transfected using RNAiMAX reagent (Invitrogen).

Tumour samples

Tumour samples were collected from ovarian carcinoma patients who consecutively underwent initial surgery at the Department of Gynecology and Obstetrics, University of Pisa, Italy. Informed consent for the experimental use of surgical samples was obtained for all patients. All specimens were sampled from the primary tumours at the time of surgery, snap frozen and stored at $-80^{\circ}C$ until use. Samples whose material was sufficient for Wb analysis were selected. Samples were homogenized in RIPA buffer supplemented with a cocktail of protease inhibitors. After initial debulking surgery, the patients were subjected to six cycles of platinum-based chemotherapy. At the end of treatment, all patients were evaluated for response to chemotherapy by physical examination, chest radiography, abdominal-pelvic, ultrasound and computerized tomography scan. Three to 5 weeks after the last course of chemotherapy, a second-look laparotomy was performed in patients with tumours of advanced stages with complete clinical response (defined as the disappearance of all signs of tumour), according to standard procedures. Complete pathologic response (remission) was defined by the disappearance of all tumour deposits with negative peritoneal washing and negative multiple random biopsies during the second look. Patients showing a partial response, a stable disease or a progressive disease were considered as no responsive to therapy (resistance). Partial pathologic response refers to a reduction of more than 50% of tumour in all measurable lesions. A stable disease refers to a reduction of $<50\%$ or to an increase of $<25\%$ in the neoplastic disease. Progressive disease refers to an increase of $>25\%$ in the size of existing lesions or to the appearance of new tumour lesions.

Genomic analysis of the TP53 gene

Genomic DNA was extracted from tumour tissues according to standard procedures. Genetic analysis of the *TP53* gene was performed by PCR amplification of exons 4–9 with flanking intronic primers followed by sequencing of positive cases.

Quantitative real-time polymerase chain reaction

Total RNA was extracted with Trizol (Invitrogen Corporation, Carlsbad, CA), according to the manufacturer's instructions. The expression of MDM4 in tumours was measured by quantitative RT–PCR, based on TaqMan methodology, using the ABI PRISM 7500 Sequence Detection System (Applied Biosystems, Foster City, CA) (Giglio *et al*, 2005). The MDM4 primers were chosen in a region not present in the variant forms MDM4-S, HDMX-G MDM4-211, XALT1 and XALT2 to amplify specifically the full-length (fl) product. The primer/probe set for MDM4 was as follow: Forward: 5′-TCGCACA GGATCACAGTATGG-3′; Reverse: 5′-TTCTTTTTCTGGAAGTGGAAC TTTC-3′; TaqMan probe: MDM4: ATTCCAAGTCAAGACCAACTGA AGCAAAGTGC.

Analysis of MDM4-S was driven by quantitative RT–PCR according to Bartel *et al* (2005).

Statistical analysis

The relationship between *MDM4* mRNA levels and cisplatin responsiveness was analysed by a two-tailed Student *t*-test. A $P<0.05$ was considered as significant. Statistic analysis was carried out using the Analyse-it software for Microsoft Excel (Analyse-it Software, Ltd).

Supplementary data

Supplementary data are available at *The EMBO Journal* Online (http://www.embojournal.org).

Acknowledgements

The authors thank Dr G Lozano for $p53^{-/-}Mdm2^{-/-}$MEFs, Dr JC Marine for $p53^{-/-}Mdm4^{-/-}$MEFs, Dr AG Jochemsen for monoclonal anti-MDM4 antibody 6B1A, Dr L Mayo for p53Ser46D expressing plasmid. We are grateful to S Bacchetti and G Deidda for critical reading of this manuscript and useful suggestion. This work was supported by grants from AIRC, Ministero della Salute, Ministero della Università e Ricerca and Regione Lazio/Distretto Tecnologico delle Bioscienze. F. Mancini was a recipient of an FIRC fellowship.

Conflict of interest

The authors declare that they have no conflict of interest.

References

Arima Y, Nitta M, Kuninaka S, Zhang D, Fujiwara T, Taya Y, Nakao M, Saya H (2005) Transcriptional blockade induces p53-dependent apoptosis associated with translocation of p53 to mitochondria. *J Biol Chem* **280:** 19166–19176

Ashcroft M, Taya Y, Vousden KH (2000) Stress signals utilize multiple pathways to stabilize p53. *Mol Cell Biol* **20:** 3224–3233

Barboza JA, Iwakuma T, Terzian T, El-Naggar AK, Lozano G (2008) Mdm2 and Mdm4 loss regulates distinct p53 activities. *Mol Cancer Res* **6:** 947–954

Bartel F, Schulz J, Bohnke A, Blumke K, Kappler M, Bache M, Schimdt H, Wurl P, Taubert H, Hauptmann S (2005) Significance of HDMX-S (or MDM4) mRNA splice variant overexpression and HDMX gene amplification on primary soft tissue sarcoma prognosis. *Int J Cancer* **117:** 469–475

Behrens BC, Hamilton TC, Masuda H, Grotzinger KR, Whang-Peng J, Louie KG, Knutsen T, McKoy WM, Young RC, Ozols RF (1987) Characterization of a cis-diamminedichloroplatinum(II)-resistant human ovarian cancer cell line and its use in evaluation of platinum analogues. *Cancer Res* **47:** 414–418

Cereghetti GM, Scorrano L (2006) The many shapes of mitochondria death. *Oncogene* **25:** 4717–4724

Chang NS, Chang NS, Doherty J, Ensign A, Schultz L, Hsu LJ, Hong Q (2005) WOX1 is essential for tumor necrosis factor-, UV light-, staurosporine-, and p53-mediated cell death, and its tyrosine 33-phosphorylated form binds and stabilizes serine 46-phosphorylated p53. *J Biol Chem* **30:** 43100–43108

Chavez-Reyes A, Parant JM, Amelse LL, de Oca Luna RM, Korsmeyer SJ, Lozano G (2003) Switching mechanisms of cell death in mdm2- and mdm4-null mice by deletion of p53 downstream targets. *Cancer Res* **63:** 8664–8669

Chipuk JE, Green DR (2006) Dissecting p53-dependent apoptosis. *Cell Death Differ* **13:** 994–1002

Chipuk JE, Kuwana T, Bouchier-Hayes L, Droin NM, Newmeyer DD, Schuler M, Green DR (2004) Direct activation of Bax by p53 mediates mitochondria membrane permeabilization and apoptosis. *Science* **303:** 1010–1014

Deng X, Gao F, Flagg T, Anderson J, May S (2006) BCL2's flexible loop domain regulates p53 binding and survival. *Mol Cell Biol* **26:** 4421–4434

D'Orazi G, Cecchinelli B, Bruno T, Manni I, Higashimoto Y, Saito S, Gostissa M, Coen S, Marchetti A, Del Sal G, Piaggio G, Fanciulli M, Appella E, Soddu S (2002) Homeodomain-interacting protein kinase-2 phosphorylates p53 at Ser 46 and mediates apoptosis. *Nat Cell Biol* **4:** 11–19

Dumont P, Leu JI, Della Pietra III AC, George DL, Murphy M (2003) The codon 72 polymorphic variants of p53 have markedly different apoptotic potential. *Nat Genet* **33:** 357–365

Tanimura S, Ohtsuka S, Mitsui K, Shirozu K, Yoshimura A, Ohtsubo M (1999) MDM2 interacts with MDMX through their RING finger domains. *FEBS Lett* **447:** 5–9

Toledo F, Krummel KA, Lee CJ, Liu CW, Rodewald LW, Tang M, Wahl GM (2006) A mouse p53 mutant lacking the proline-rich domain rescues Mdm4 deficiency and provides insight into the Mdm2-Mdm4-p53 regulatory network. *Cancer Cell* **9:** 273–285

Toledo F, Wahl GM (2006) Regulating the p53 pathway: *in vitro* hypotheses, *in vivo* veritas. *Nat Rev Cancer* **6:** 909–923

Wade M, Wahl GM (2009) Targeting Mdm2 and Mdmx in cancer therapy: better living through medicinal chemistry? *Mol Cancer Res* **7:** 1–11

Xiong S, Van Pelt CS, Elizondo-Fraire AC, Liu G, Lozano G (2006) Synergistic role of Mdm2 and mdm4 for p53 inhibition in central nervous system development. *Proc Natl Acad Sci USA* **103:** 3226–3231

Yang X, Fraser M, Moll UM, Basak A, Tsang BK (2006) Akt-mediated cisplatin resistance in ovarian cancer: modulation of p53 action on caspase-dependent mitochondria death pathway. *Cancer Res* **66:** 3126–3136